SPEED CONTROLLER DESIGN FOR A VECTOR-CONTROLLED PERMANENT MAGNET SYNCHRONOUS

MOTOR DRIVE WITH PARAMETER VARIATIONS

Juan C. Balda
University of Arkansas
Fayetteville, AR 72701

Pragasen Pillay
University of Newcastle
England, NE1 7RU, UK

ABSTRACT ~ If classical techniques such as the root locus, Bode plots and Nyquist diagrams are used for designing fixed-structure speed controllers for ac drives, the design would normally be done around a nominal value of the controlled plant. Generally, a sensitivity analysis would subsequently be done to ensure that the design specifications are met when the plant parameters change. This procedure can and has worked well. In this paper an alternative is proposed where the parameter variations are included at the outset of the design task. The Nichols chart lends itself rather well to this application since it represents both magnitude and phase information on a single diagram. By using this alternative, it may be possible to reduce the overall time needed to complete the design. The particular technique is called Quantitative Feedback Theory (QFT) which is used in conjunction with the Nichols chart. This paper presents the basics of QFT and shows how it can be used for the design of fixed-structure controllers for parameter-sensitive plants in conjunction with the Nichols chart. A design is presented and verified experimentally.

I. INTRODUCTION

The permanent magnet synchronous motor (PMSM) which by definition here has a sinusoidal back emf [1], is establishing itself as a serious competitor to the vector-controlled induction motor (IM) and the dc motor for high performance speed and position applications. This is partly due to the increased torque to inertia ratio and power density [2,3] when compared to the IM or the dc motor, in the fractional to 30 HP range. This has been made possible by the use of high residual flux density/high coercivity permanent magnets. Current research into reducing the temperature dependence and increasing the thermal capability of magnets will probably increase the penetration of the PMSM drive in the servo industry.

The high performance attainable from the PMSM has prompted original research into the design and performance of the entire motor drive including the motor [4], position and speed feedback [5], inverter, current, speed and position controllers. The application of a PMSM to an electric vehicle has been examined [6] while high speed operation has also been investigated [7,8].

In order to extract the best performance from a given machine, the proper design of the speed and current controllers (for a speed servo) is important. However all drives are parameter sensitive to some degree. Traditional methods of controller design in the frequency domain use a nominal value of the plant parameters. The effects of changes in the parameters can be subsequently checked by a sensitivity analysis [9,10]. This method can work well, however an alternative is proposed in this paper for the design of fixed-structure speed controllers [11,13] for a high performance drive. This consists essentially of including information on the drive parameter variations at the outset so that the performance criteria can be met from the beginning, without having to subsequently do a sensitivity analysis. This should reduce the effort and time of the designer without compromising the design.

Whereas design tools like the root locus, Bode plots and Nyquist diagrams have been used extensively in controller design, the Nichols chart lends itself rather well to the particular problem of representing parameter variations in a drive. The Nichols chart represents both phase and magnitude information on the same diagram unlike Bode plots which represent them separately.

This paper demonstrates how a frequency-domain technique known as 'Quantitative Feedback Theory' may be applied to the design of fixed-structure speed controllers for a vector-controlled PMSM drive where the motor parameters vary between known limits. The parameter variations can be caused by changes in temperature, current level or operating frequency. In robotic applications, changes in inertia occur as well. Finally, another source of uncertainty is the fact that the parameters of the 'Nominal Plant' are normally measured (calculated) with a certain error which is generally expressed as a percentage of the 'nominal' parameter value.

The aim of this paper is two-fold. Firstly, the elements of QFT are revised and it is then shown how QFT can be applied to the design of fixed-structure controllers for parameter-sensitive plants. In this case, the paper is tutorial in nature. Furthermore, a speed controller design is presented and verified experimentally. This is the second contribution of this paper.
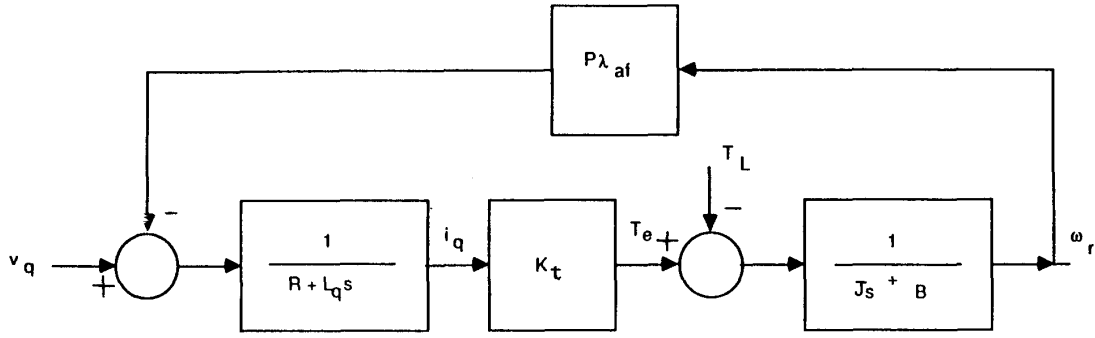
Figure 1   Schematic of a permanent magnet synchronous motor.

II. MATHEMATICAL MODEL - TRANSFER FUNCTION OF A PMSM DRIVE WITH PARAMETER VARIATIONS

Mathematical Model

Simplifications occur in the modeling of a PMSM under vector control which result in a linear transfer function between the output and commanded speeds. This can be derived from the PMSM d,q equations as follows:

$$v_q = R_s i_q + p\lambda_q + \omega_e \lambda_d \tag{1}$$

$$v_d = R_s i_d + p\lambda_d - \omega_e \lambda_q \tag{2}$$

$$T_e = (3/2) \ P \ (\lambda_{af} i_q + (L_d - L_q) i_d i_q) \tag{3}$$

$$T_e = T_L + B \ \omega_r + J \ p\omega_r \tag{4}$$

$$\omega_e = P \ \omega_r \tag{5}$$

where v_d, v_q are the d,q axis voltages; λ_d, λ_q are the d,q axis flux linkages; i_d, i_q are the d,q axis currents, P is the number of pole pairs; p is the derivative operator; L_d, L_q are the d,q axis inductances, T_e is the electric torque, T_L is the load torque, B is the damping coefficient and J is the moment of inertia. The electric speed ω_e is related to the mechanical speed through the number of pole pairs. Finally λ_{af} is the mutual flux between the magnet and the stator due to the magnet and

$$\lambda_d = L_d i_d + \lambda_{af} \tag{6}$$

$$\lambda_q = L_q i_q \tag{7}$$

Equations (1) to (3) are nonlinear but if vector control [3] is used to force i_d to be zero, then using (6) and (7), (1) to (3) reduce to

$$v_q = R_s i_q + L_q p i_q + \omega_e \lambda_{af} \tag{8}$$

$$v_d = -\omega_e L_q i_q \tag{9}$$

$$T_e = (3/2) \ P \ \lambda_{af} i_q = K_t i_q \tag{10}$$

where K_t is the torque constant of the PMSM; the above equations are very similar to that of a dc motor. It is only necessary to include the dynamics of i_q in the model since the electric torque depends only on i_q. From equations (8), (10) and (4) the linear block diagram in Fig. 1 can be drawn.

A PMSM speed servo drive is obtained from Fig. 1 by including the speed and current controllers as shown in Fig. 2 (Note that all commanded values are indicated with an '*'). The current controller is used to ensure that the actual current tracks the commanded current while the speed controller does the same for the speed. Current and speed feedback is normally used as shown in Fig. 2. For a given configuration of the current controller, the block diagrams to the right of the dotted line constitute the controlled plant P(s) and the aim of this paper is the proper design of $G_1(s)$ under uncertainties and parameter variations in P(s).
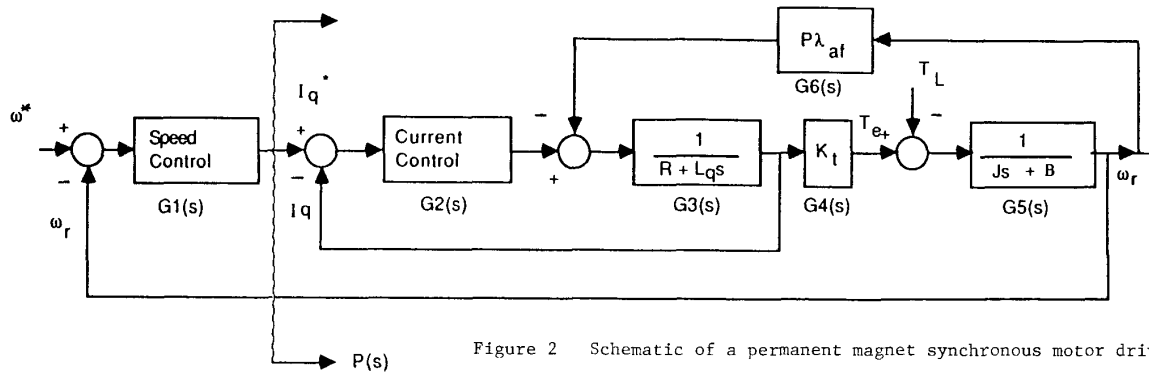

Figure 2   Schematic of a permanent magnet synchronous motor drive.

164

Parameter Variations

Assuming that the current controller gains are set correctly, parameter uncertainties are then produced in $G_3(s)$, $G_4(s)$, $G_5(s)$ and $G_6(s)$ which represent the machine as a result of changes in the temperature, current level, inertia and operating frequency. For example, changes in the temperature affect the stator resistance R_s and magnet flux linkage λ_{af} which in turn affects K_t. Changes in the current can saturate L_q while changes in frequency can affect R_s but generally to a lesser extent than changes in the temperature [10]. In robotics, inertia changes also occur which will affect $G_5(s)$. The criteria for choosing the range of variation for the parameters is presented in Ref. [10] and include the flux loss coefficient of the magnet and the degree of saturation for the machine. This paper has also included the tolerance in the 'Nominal Plant' parameters due to measurement (calculation) errors. The ranges of parameter variations are given in Table I as a fraction of the nominal value which is at ambient temperature.

Transfer Function

From Fig. 2, the plant transfer function P(s) is given by

$$\frac{\Omega_r(s)}{I_q^*(s)} = \frac{b_1 s + b_0}{s^3 + a_2 s^2 + a_1 s + a_0} \qquad (11)$$

which can be attained from block diagram reduction or Mason's rule/signal flow graphs. From an analysis of the parameter variations shown in Table I, the variations of the coefficients of P(s) are as follows:

TABLE II.   COEFFICIENT VARIATIONS IN P(s)

	Nominal	Minimum	Maximum
b_1	1941783.10	470513.74	3814859.20
b_0	8.7865e+09	2.129e+09	1.7262e+10
a_3	1.0	1.0	1.0
a_2	9771.01	7504.11	17479.11
a_1	44703871.0	33647342.0	80291919.0
a_0	7026177.70	2702403.20	12548858.0

III. BASICS OF QFT

This section only reviews some of the main theoretical concepts of QFT since it has been extensively published elsewhere [11-13]. Consider the regulating feedback system shown in Fig. 2 whose output equation is given by:

TABLE I.   PARAMETER VARIATIONS FOR AC DRIVE

$0.90 \leq R_s \leq 1.1$ (0.12 ohms)
$0.63 \leq \lambda_{af} \leq 1.1$ (1.513 V/rad/sec)
$0.56 \leq L_q \leq 1.3$ (0.764 mH)
$0.63 \leq K_t \leq 1.1$ (6.807 N-m/Amps)
$1.00 \leq J \leq 2.0$ (0.0337 Kg-m^2)

Numerical values are presented as fractions of nominal values which are between brackets.

$$\Omega_r(s) = \frac{L(s)}{1 + L(s)} \Omega_r^*(s) \qquad (12)$$

where $\Omega_r(s)$, $\Omega_r^*(s)$ are the Laplace transforms of ω_r and ω_r^* respectively, $L(s) = G_1(s)P(s)$ is the loop transfer function, and P(s) is the plant whose parameter variations are shown in Table II.

An analysis of (12) shows that the design objective is that the plant output $\Omega_r(s)$ follows the input signal $\Omega_r^*(s)$ as closely as possible. Since one of the aims of this paper is to illustrate the feasibility of the QFT approach to design a fixed-structure speed controller for ac drives, the design task has been simplified by not considering the influence of any sensor noise or disturbance. However, it must be clear that this does not represent a limitation of this design technique since any spurious signal can also be considered [13].

The design is done on the Nichols chart which is shown in Fig. 3; the x-axis represents phase (in degrees),the y-axis represents magnitude (in dB) and a background (dotted lines) is included which corresponds to constant phase (or magnitude) curves of [L(s)/(1+L(s))]. The Nichols chart presents the advantage that the loop transfer function $L(j\omega) = G_1(j\omega)P(j\omega)$ may be easily drawn from a knowledge of $P(j\omega)$ by just adding the magnitude (in dB) and the phase (in degrees) of $G_1(j\omega)$ to the magnitude and phase of $P(j\omega)$ for each relevant frequency (the point $P(j\omega)$ is then translated but not rotated).

The uncertainty of P(s) is considered in the same way as in the tracking designs of Horowitz [11,12]. The regulator problem is to maintain $|L(s)/(1+L(s))|$ below a specified limit at specified frequencies for all possible P(s) (see Table II). Of all P(s), the designer usually chooses an arbitrary $P_0(s)$ which corresponds to the so-called 'Nominal Plant'.
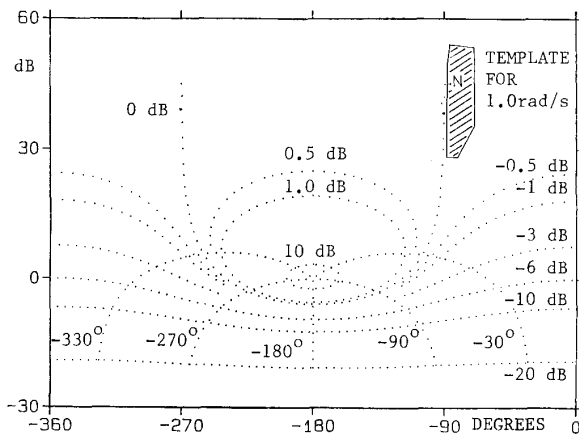
Figure 3   Nichols chart with the plant template for **1.0** rad/s.

The 'plant templates' are then fitted between certain $|L(j\omega)/(1+L(j\omega)|_{dB}$ curves (boundaries) around the Nyquist point (-180°, 0 dB) as shown in the next section. A 'plant template' is the loci of points corresponding to all $P(j\omega)$ considered in the uncertainty range (shown Table II) for a given frequency ω. Due to space limitations, only one typical template of $P(j\omega)$ for $\omega = 1.0$ rad/s (0.159 Hz) is shown in Fig. 3 as a shaded area; the point corresponding to the 'Nominal Plant' is represented by the letter 'N'.

In a QFT design, the structure of the controller is not fixed apriori but evolves as part of the design process. In this way it is guaranteed that no over- or under-design of the controller occurs. Disadvantages of the QFT are that it is not always possible to establish the uncertainty range of $P(s)$ quantitatively and correlation between time- and frequency-domain specifications is a sort of an art; but so is much of design.

IV. SYSTEMATIC DESIGN OF THE SPEED CONTROLLER

The design task chosen was to select a $G_1(s)$ which ensures that the closed loop response

$$| L(j\omega)/(1+L(j\omega)) | \leq 1.0 \text{ dB} \qquad (13)$$

for all frequencies below 150.0 rad/s and for all possible $P(j\omega)$ (see Table II). The 1.0 dB criterion was chosen arbitrarily and the steady-state speed error must be zero since this plant is a speed servo. Although these specifications were set arbitrarily, the designer can specify other constraints according to the application of the drive.

The following steps are carried out in order to achieve the design specifications:

a)   Obtain the templates of $P(s)$ for the range of frequencies which are of interest (see Fig. 3 for the template corresponding to 1.0 rad/s).

b)   Determine a boundary of the 'Nominal Plant' $P_o(j\omega)$ with $G_1(j\omega) = 1.0$ in the Nichols chart at each relevant frequency ω. This is done by shifting the template corresponding to a specific frequency ω (see Fig. 3) around the 1.0 dB curve such that NO POINT within the template falls inside the 1.0 dB curve (see section III: no rotation of the template must occur, only vertical and/or horizontal displacements). The point within the template which corresponds to $P_o(j\omega)$ (N in Fig. 3) traces out a boundary of $L_o(j\omega)$ at the considered frequency ω. Figure 4 depicts some of the boundaries thus obtained with the specific frequency being encircled. Finally, the 1.0 dB curve is considered here because this is one of the design specifications (see (13)).

c)   Design a controller for the 'Nominal Plant' $P_o(s)$ using the Nichols chart. The design must guarantee that the value of the loop transfer function $L_o(j\omega)$ (i.e. $P_o(j\omega)$ and designed $G_1(j\omega)$) for any particular frequency ω is outside the boundary for that frequency. Then any other $L(j\omega)$ (i.e. for any other $P(j\omega)$ within Table II) also meet the design specifications at that particular frequency ω. This is true because the boundaries of $P_o(j\omega)$ were obtained such that NO POINT of the template (all considered $P(j\omega)$) falls within the 1.0 dB curve for the considered frequency (Remember that the magnitude of $L(j\omega)$ in the Nichols chart is equal to the sum of the magnitudes of $P(j\omega)$ and $G_1(j\omega)$ in dB, and the phase of $L(j\omega)$ is the sum of the phases of $P(j\omega)$ and $G_1(j\omega)$ in degrees). In other words, if the 'Nominal Plant' $P_o(s)$ with the designed controller $G_1(s)$ satisfies all specifications, it is then concluded that all $P(s)$ in Table II must also satisfy the specifications [11,12].

Figure 4 shows the loci of the loop transfer function $L_o(s)$ for the 'Nominal Plant' with:

$$G_1(s) = \frac{\Omega_r(s)}{\Omega_r^*(s)} = \frac{5 (1 + s/5)}{s (1 + s/600)(1 + s/2000)} \qquad (14)$$

where $G_1(s)$ is the result of following the above steps in an interactive manner. The low-pass filters at 600 and 2000 rad/s are required to reduce high frequency noise. From an analysis of Fig. 4, it can be noted that the point $L_o(j10)$ just satifies the boundary for $\omega = 10.0$ rad/s; all other relevant points amply satisfy the design requirements.
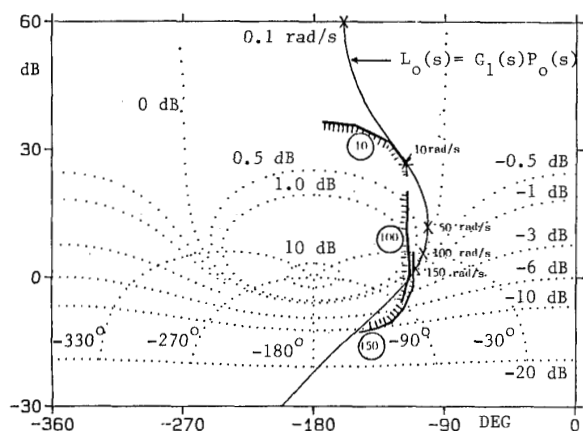
Figure 4 1.0 dB design limits (see (13)) at 10, 100 and 150 rad/s together with the loop transfer function for the 'Nominal Plant' $P_o(s)$ and the controller $G_1(s)$ (see (14)).

Finally, this design procedure is suitable for computer implementation in an interactive manner; the user can graphically note if a controller satisfies the specifications and modify the design if necessary.

V. RESULTS

In order to test the design technique, a design was done on a motor with parameters presented under motor A in Table III but actually implemented on motor B which had different parameters within the uncertainty range considered in Table II.

TABLE III.   PMSM DATA

Parameter	Motor A	Motor B
HP	8.9	9.4
rated speed (rpm)	1350	1450
rated torque (N-m)	47.1	46.2
K_t (N-m/amps RMS)	2.39	2.18
back emf (V_{ll}/rpm)	0.144	0.11
R_s @ 25°C (Ω)	1.08	1.165

The speed controller $G_1(s)$ described previously was implemented using analog circuits. Without any further tuning, the controller was tested by commanding a speed of 520 rpm. The startup speed transient is shown in Fig. 5. There is a slight overshoot which was allowed for in the design.

Figure 6 shows the Bode plots of the entire drive including the controller; the speed loop bandwidth is approximately 250 rad/s. If a higher bandwidth is needed, this can be included as part of the specifications.
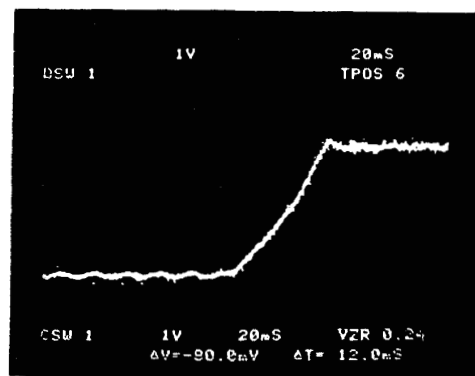

Figure 5   Start-up speed response with the designed speed controller.
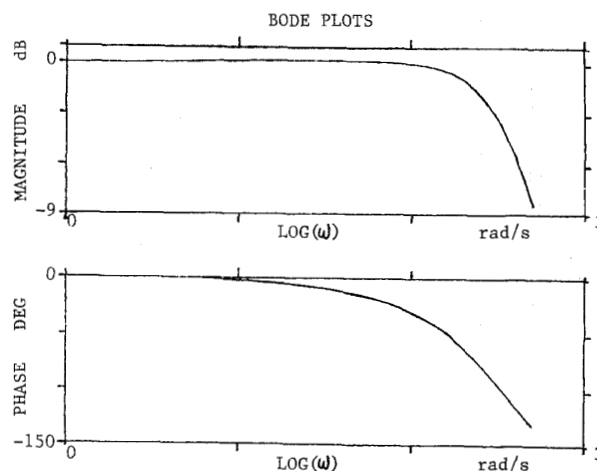

Figure 6   Bode plots of the motor drive with the designed speed controller (see (14)).

A key test of the performance of a speed servo is its response to a load torque disturbance. Indeed if rejection capabilities to a load torque disturbance are judged to be of prime importance, the speed controller design can be done with this specification in mind. To examine the performance of the speed controller to load torque disturbances, the transfer function of (Ω_r/T_L) was developed and its Bode plots are shown in Fig. 7. The high attenuation, even at 1.0 rad/s and which increases as the frequency of T_L is increased, attests to the extremely good load rejection capabilities of the speed controller. The high attenuation implies that the actual speed does not respond well to load torque inputs, which is highly desirable.

In addition to the response of the speed to a changing load torque input, the steady-state error in the speed due to a step input in the load torque was examined. For a 1.0 p.u. input torque, there is a reduction in 2.9% in the full load speed.
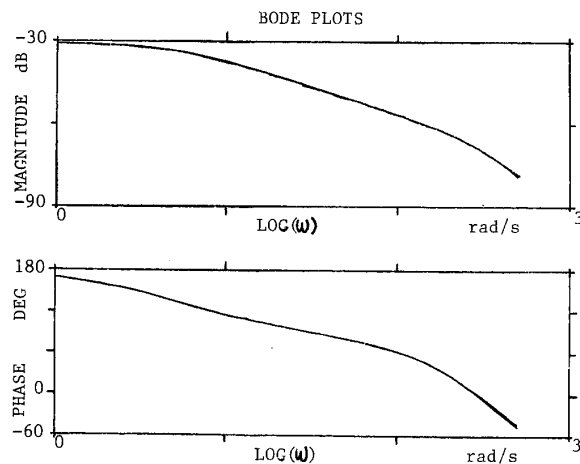
167

BODE PLOTS

Figure 7 Frequency response of the motor drive to load disturbances (Ω_r/T_L).

Zero steady-state error is difficult if not impossible to obtain due to the practical difficulties of implementing a pure integrator. In practice, it is generally necessary to implement the integrator pole close to the $j\omega$ axis and so the pure integrator is actually implemented as a low pass filter and hence with some steady-state error.

VI. CONCLUSIONS

This paper has illustrated how Quantitative Feedback Theory can be used in conjuntion with the Nichols chart to design a fixed-structure speed controller for a PMSM drive. Parameter variations were taken into account in the initial stages of the design which is conducted such that even in the worst case, the design specifications are met. Parameter variations due to temperature, saturation, operating frequency and change in inertia were considered. A systematic procedure for the controller design was also given.

In order to check the ability of the controller to perform in the presence of parameter variations, the design was conducted with one set of motor parameters but implemented on another motor whose parameters were within the uncertainty range of the first. The practical results were satisfactory thus validating the design procedure and implementation. The speed loop Bode plots and load rejection capabilities were also examined and found to be acceptable as was the steady-state speed error due to the practical difficulties of implementing a pure integrator.

VII. ACKNOWLEDGEMENTS

VIII. REFERENCES

[1] G. Pfaff, A. Weschta and A. Wick, 'Design and Experimental Results of a Brushless ac Servo Drive', 1981 Annual Meeting IEEE-IAS., 1981, pp. 692-697.

[2] R. Krishnan, 'Selection Criteria for Servo Motor Drives', IEEE Trans. on IA, Vol. IA-23, No. 6, 1987, pp. 270-275.

[3] P. Pillay and R. Krishnan, 'Modeling, Analysis and Simulation of a High Performance, Vector-Controlled, PMSM Drive', 1987 Annual Meeting IEEE-IAS, 1987, pp. 253-261.

[4] N. Boules, 'Prediction of no load Flux Density Distribution in Permanet Magnet Machines', 1984 Annual Meeting IEEE-IAS, 1984, pp. 464-473.

[5] E.K. Persson, 'Brushless DC Motor - A Review of the State of the Art', Conf. Rec. 1981 Motorcon Conf., pp. 1-16.

[6] B.K. Bose, 'A High Performance Inverter-Fed Drive System of an Interior Permanent Magnet Synchronous Machine', 1987 Annual Meeting IEEE-IAS., 1987, pp. 267-276.

[7] T.M. Jahns, 'Flux Weakening Regime Operation of an Interior Permanent Magnet Synchronous Motor Drive', 1986 Annual Meeting IEEE-IAS, 1986, pp. 814-823.

[8] T. Sebastian and G.R. Slemon, 'Operating limits of Inverter-Driven Permanent Magnet Motor Drives', 1986 Annual Meeting IEEE-IAS, pp. 800-805.

[9] G.F. Franklin, J.D. Powell and A. Emami-Nacini, 'Feedback Control of Dynamic Systems', (book).

[10] R. Krishman and P. Pillay, 'Parameter Sensitivity in Vector Controlled AC Motor Drives', 1987 IEEE IECON, pp. 252-218.

[11] I. Horowitz and M. Sidi, 'Synthesis of Feedback Systems with Large Plant Ignorance for Prescribed Time-Domain Tolerances', Int. J. Control, Vol. 16, No. 2, 1972, pp. 287-309.

[12] I. Horowitz, S. Oldak and O. Yaniv, 'An Important Property of Non-Minimum-Phase Multiple-Input-Multiple-Output Feedback Systems', Int. J. Control, Vol. 44, No. 38, 1986, pp. 677-688.

[13] E. Eitelberg, J.C. Balda, E.S. Boje and R.G. Harley, 'Stabilizing SSR Oscillations with a Shunt Reactor Controller for Uncertain Levels of Series Compensation', IEEE Transactions on Power Systems, Vol. 3, No. 3, August 1988, pp. 936-943.